Int. J. Appl. Ceram. Technol., 13 [5] 821–830 (2016)
DOI:10.1111/ijac.12557

Additive Manufacturing of Dense Ceramic Parts via Direct Ink Writing of Aqueous Alumina Suspensions

Lisa Rueschhoff, William Costakis, Matthew Michie, Jeffrey Youngblood, and Rodney Trice*

School of Materials Engineering, Purdue University, 701 W. Stadium Ave, West Lafayette, 47907, Indiana

Additive manufacturing of near-net-shaped dense ceramic components has been established via room-temperature direct writing of highly loaded aqueous alumina suspensions in a layer-by-layer fashion. The effect of alumina solid loading on rheology, specimen uniformity, density, microstructure, and mechanical properties was studied. All suspensions contained a polymer binder (~5 vol.%), dispersant, and 51–58 vol.% alumina powder. Rheological measurements indicated all suspensions to be yield-pseudoplastic, and both yield stress and viscosity were found to increase with increasing alumina solid loading. Shear rates ranging from 19.5 to 24.2/s, corresponding to viscosities of 9.8 to 17.2 Pa·s, for the 53–56 vol.% alumina suspensions were found to produce the best results for the 1.25-mm tip employed during writing. All parts were sintered to >98% of true density, with grain sizes ranging from 3.2 to 3.7 μm. The average flexure strength, which ranged from 134 to 157 MPa, was not influenced by the alumina solid loading.

Keywords: *rheology/rheometry; alumina; processing; printing*

Introduction

Additive manufacturing is gaining momentum in all areas of materials research due to the ability to create three-dimensional parts directly from CAD designs through adding materials layer by layer, producing near-net shape complex geometries that would not be possible with subtractive manufacturing.[1] Emerging technologies in ceramic-additive manufacturing include direct-write assembly of ceramics from colloidal inks by both droplet-based and continuous or filament-based approaches.[2] Droplet-based direct-write assembly includes processes such as direct inkjet printing and hot-melt printing, in which low solid content (~5 vol.%) droplets are deposited into a desired pattern in a layer-by-layer build sequence.[2] The starting materials, or inks, used in this process consist of dye-based inks in a low-viscosity fluid or wax-based system.[2] While a variety of compositions are used, often upwards of 50 vol.% of the system is organic content, which demands lengthy binder removal steps that result in large dimension changes.[2] As the process is not continuous, total forming time is limited by the time to print each droplet. On the other hand, filament-based direct-write approaches such as fused deposition,[3] freeze-form extrusion fabrication,[4] free-form fabrication,[5] and robocasting[6,7] have also been used to form complex shapes and rely on the continuous extrusion of a highly concentrated (>45 vol.%) colloidal ink through a nozzle in a layer-by-layer sequence.[8] In these filament-based approaches, the highly loaded colloidal ink is extruded through a small cylindrical nozzle to create a filamentary element that is deposited in a layer-by-layer sequence.[9]

Direct ink writing using a continuous filament will be explored further in this study as a means to produce three-dimensional components using computer-controlled layer-by-layer deposition of a highly loaded colloidal suspension. This process was chosen for its ability to form near-net and complex shapes of easily densified ceramic parts due to the use of highly concentrated suspensions. The use of a low-cost syringe style 3D printer will be explored as a means to perform layer-by-layer deposition to form near-net-shaped ceramic parts.

Using a previously developed suspension formulation,[10–12] ceramic suspensions composed of a ceramic powder, dispersant, polymer binder, and water can be utilized for direct writing complex ceramic objects. Alumina has been used in preliminary experiments as a model material due to its low cost, availability, and ease of densification. Previous studies[10,11] have optimized alumina suspensions using PVP as a binder and a cationic polyelectrolyte as a dispersant. In prior work,[10] PVP has been shown to increase green body strength and machinability of alumina parts prepared by room-temperature injection molding. Unlike gel casting and other similar fabrication techniques, using PVP does not require cross-linking or elevated temperatures for formation.

These alumina suspensions show yield-pseudoplastic behavior, a term describing a material that is shear

*rtrice@purdue.edu

thinning after overcoming a yield stress. This behavior allows the suspensions to easily flow under the shear stress of deposition (after overcoming a yield stress) and to retain its shape once the stress is removed. This retention of shape allows multiple layers to be deposited on top of each other. The use of PVP will not only allow for more robust and machinable green bodies, but will also offer unique flow properties that can be more precisely tailored for this process. Preliminary research found that for a 50 vol.% alumina suspension a threefold increase in yield stress was obtained when adding just 1 vol.% of PVP (55,000 g/mol).[11] Injection molding studies on these alumina suspensions found 2.5–5.0 vol.% of PVP (55,000 g/mol) to provide adequate yield stresses and viscosities needed to form robust, machinable green bodies.[10] Both of these studies explored a large range of PVP molecular weights and contents, resulting in a vast variety of flow properties, asserting the ability to tailor these suspensions.

In this study, we have investigated the use and benefit of our tailored alumina suspensions in the direct writing process with the underlying design principle of maximizing solid loading while not compromising the quality of formed specimens. Rheology and uniformity in deposited layers were used to assess the effect of different alumina powder loadings on a standard formed part. The effect of alumina solid loading on physical properties (density and microstructure) and mechanical properties was investigated.

Experimental Approach

Alumina suspensions used in this study were produced using reverse osmosis (RO) water and grade A-16 SG alumina (Almatis, New Milford, CT), which was previously determined[10] to have a BET surface area of 7.8 ± 0.22 m^2/g and an average particle size of 0.48 ± 0.13 μm using a Beckman Coulter LS 230 particle size analyzer (Brea, CA). Darvan 821A (R.T. Vanderbilt Company, Norwalk, CT), a low-toxic aqueous solution of 40 wt.% ammonium polyacrylate (PAA-NH_4) with a molecular weight of 3500 g/mol,[13] was used as a dispersant in order to optimize particle stability in the suspension. A water-soluble room-temperature flowable 55,000 g/mol polyvinylpyrrolidone (PVP, 1-ethenyl-2-pyrrolidinone homopolymer; Sigma-Aldrich, St. Louis, MO) was used to alter the rheological properties of the suspension and the mechanical strength of the green bodies. Previous work on these aqueous alumina suspensions found the addition of and increase in added PVP caused an increase in both viscosity and yield stress.[11,12] An aqueous slurry of RO water and PVP was prepared by mixing on a stir plate for 12 h. A stand mixer with spindle attachment (VWR International, Radnor, PA) was used to prepare the alumina suspensions through gradually adding alumina powder and dispersant to the mixed polymer slurry at rates increasing from 200 to 450 rpm to achieve the highly loaded suspensions. After mixing, the suspensions were left on a ball mill to stay homogenized until they were used for forming or testing, typically <5 h. Solid loading in the suspensions were varied to include 51, 53, 55, 56, and 58 vol.% alumina in order to optimize the rheological properties for the direct writing process to form specimens with high sintered densities and mechanical properties. All suspensions were made with approximately 5 vol.% PVP and 4 vol.% dispersant, with exact compositions for each suspension investigated listed in Table I. To increase the volumetric solid loading of the suspensions, more alumina was added to the stock solution, leading to a decrease in the volume fraction of the other constituents.

A Malvern Bohlin Gemini HR rheometer (Malvern Instruments, Worcestershire, UK) with a 25-mm cup

Table I. Compositions of Alumina-PVP Suspensions with Corresponding Herschel–Bulkley Curve Fitting Parameters for Yield-Pseudoplastic Fluids. Nominal Viscosity During Forming was Calculated Based on Measured Shear Rates During Forming for Each Suspension, and Average Layer Height was Measured from Green Body Specimens Formed via Direct Writing

Al_2O_3 (vol.%)	Dispersant (vol.%)	PVP MW = 55k (vol.%)	σ_y (Pa)	k (Pa·s^n)	n	Nominal viscosity during forming (Pa·s)	Average deposited layer height (mm)
51	4.5	5.3	83	16.7	0.57	7.5	0.88 ± 0.37
53	4.4	5.1	116	17.6	0.61	9.9	0.85 ± 0.14
55	4.2	4.9	157	18.7	0.64	12.8	0.85 ± 0.07
56	4.1	4.8	191	27.6	0.56	17.2	0.90 ± 0.20
58	3.9	4.5	268	19.7	0.68	25.0	0.86 ± 0.32

and bob geometry fixture and a gap of 150 μm was used to determine the rheological properties of the alumina suspensions. Approximately 13 mL of each suspension was used to test the rheology within 24 h of mixing, and a water trap was used to minimize premature drying of the suspension during testing. The maximum shear rate of each suspension during extrusion was determined using the following equation[14]:

$$\dot{\gamma} = \frac{4Q}{\pi r^3}$$

where Q is the volumetric flow rate during extrusion and r is the radius of the nozzle. Each suspension was extruded from a syringe with internal nozzle radius of 0.625 mm for a set time, and the Q value was determined by measuring the mass of material extruded and converting to volume based on density. The density of the suspensions ranged from 2.54 to 2.75 g/cm^3. Through this method, it was determined that the shear rate during extrusion ranged from 19.5/s for a 56 vol.% alumina suspension to 24.2/s for a 53 vol.% suspension.

Stress as a function of shear rate flow curves was obtained for each suspension by measuring shear stresses for controlled shear rates increased logarithmically from 0.01 to 35/s. The samples were subjected to a preshear of 100/s for 20 s to ensure maximum uniformity and a uniform shear history of the suspensions before each flow curve was obtained. The flow curves obtained for each sample were fitted to the Herschel–Bulkley model for yield-pseudoplastic fluids[15], which is defined as:

$$\sigma = \sigma_y + k\dot{\gamma}^n$$

where σ is the shear stress, σ_y is the yield stress for the material, k is the consistency index, $\dot{\gamma}$ is the applied shear rate on the material and n is the flow index that ranges from 0 to 1. A material is considered shear thinning if the flow index is <1.[16] The rheological results for the suspensions were fit to this model using a method of least squares to determine the yield stress and flow index for each.

The room-temperature direct writing process was carried out through a modified Imagine syringe 3D printer (Essential Dynamics, New York, NY) shown in Fig. 1a. The printer is equipped with a printing head fixture that holds 10-mL syringes with a metal tip with an internal diameter of 1.25 mm. The syringe moved along the x- and y-axes at 4 mm/s and the suspension was deposited in a layer-by-layer format onto a build platform that moves 0.85 mm down the z-axis with each deposited layer. The stage where the alumina suspension is deposited is covered with a level polymethylmethacrylate plate that has been wiped down with Teflon spray to ensure easy removal of dried specimens. A motor with a gear ratio of 231:1 (Snap Motors, Berkeley, CA) was used to rotate a threaded rod and plunger, forcing the suspension out of the syringe and onto the platform at a controlled rate. The printer was connected to a computer using FabStudio and FabInterpreter software (Fab@-Home project). FabStudio software was used to import 3D CAD files and create a path file that uses a predetermined algorithm to create a file that communicates the raster path for the syringe to follow. This file was imported into the FabInterpreter software that controls the motors.

The descriptions of the controllable parameters and the optimized values for the direct writing process are listed in Table II. These values were optimized with suspensions used in this study through a set of trial and error direct writing experiments. In particular, the flow output of the suspensions was decreased to obtain a steady and uniform layer of alumina suspension, which

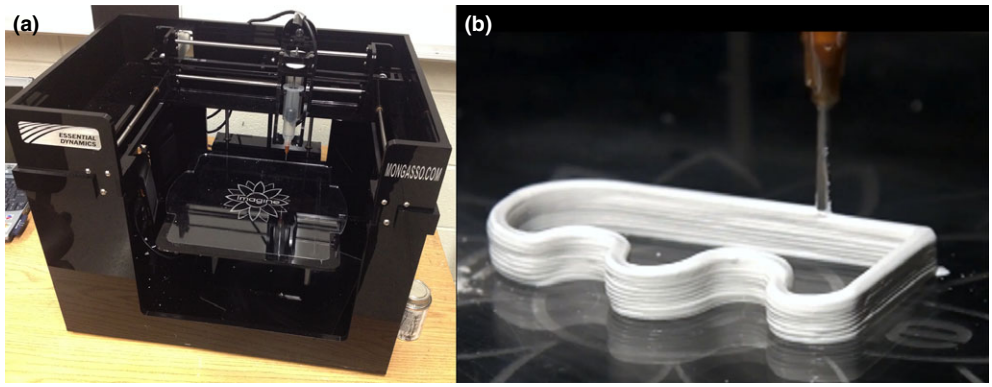

Fig. 1. (a) Imagine 3D printer from Essential Dynamics used for direct writing alumina suspensions (b) in progress deposition of a 55 vol.% alumina suspension layer by layer to form a test shape.

Table II. Alterable Variables with the Optimized Values Used for the Direct Writing Experiments Presented

Parameter	Value	Description
Slice height	0.85 mm	Set height between syringe tip and build platform
Path speed	4 mm/s	Speed of syringe fixture
Path width	1 mm	Deposited layer width
Deposition rate	0.007 mm/s	Deposition rate of suspension
Pushout	0.05 s	Time of plunger forward motion prior to the start of each layer
Suckback	0.05 s	Time of plunger backward motion at the end of each layer
Suckback delay	0 s	Delay time between end of layer and suckback
Clearance	2 mm	Height of syringe nozzle above the previously deposited layer

was achieved at a deposition (plunger) speed of 0.007 mm/s and a path (syringe) speed of 4 mm/s. Higher flow rates caused inconsistencies in the material deposition that make it harder to create more detailed and complex features. The height and width of the deposited layer were also adjusted in order to achieve maximum shape retention of the filament. Calibration of the hardware included calibrating tension of the drive belts and adjusting counts per second of the motors within the software.

To quantify the differences in density, microstructure, and mechanical properties of varying alumina solid contents in suspensions, flexural strength samples were produced for 53–56 vol.% alumina solid loading via direct writing. Previous studies of PVP burnout in air[10] showed significant weight loss between 325°C and 480°C. Therefore, the binder burnout of formed specimens was carried out in air using a tube furnace with a heat rate of 5°C/min to 700°C with a 1-h isothermal hold followed by cooling to room temperature with no controlled cooling rate. This temperature was chosen to ensure complete burnout of the polymer. A box furnace was used for pressureless sintering the specimens with a 5°C/min heat rate to 1600°C with a 1-h isothermal hold followed by cooling to room temperature.

Drying linear shrinkage of samples formed via this direct writing process was obtained by measuring the dimensions before and after drying of a 4 × 4″ square outline. Geometric green body density calculations were determined via dimensional and mass measurements on dried formed bodies of the same square outline. Average bulk density of the sintered alumina parts was determined via Archimedes method in accordance with ASTM C 373[17], and percent of true density (%TD) was calculated with TD_{Al2O3} = 3.98 g/cm^3. An XL-40 (FEI, Hillsboro, OR) scanning electron microscope (SEM) was used to analyze the microstructure of the sintered sample. Grain size calculations were conducted in ImageJ via the line intercept method by randomly placing 100 lines each 56 μm in length on a representative SEM image for each condition.

Specimens for three-point bend mechanical testing were obtained by direct writing suspensions with solid loading of 53, 55, and 56 vol.% into 4″ × 4″ square outlines with a width of two deposited layers and a height of six layers. The corners of the green body squares were cut to create four test bars per square in accordance with ASTM C1161[18] for measuring flexural strength of ceramics at ambient temperature. Sintered test bars were made into size A specimens (25 × 2 × 1.5 mm) using a longitudinal surface grinder (Supertec Machinery, Paramount, CA) and surface-polished using 320, 400, and 600 grit SiC paper, and 3 and 6 μm diamond paste. A custom-made semi-articulating testing fixture was made with stainless steel in accordance with size A for the ASTM C1161 standard, which has a support span of 20 mm and cylindrical bearings of approximately 2 mm diameter. The fixture was assembled between two faced-off stainless steel platens in an electromechanical test frame (MTS Insight 100 load frame; MTS Systems, Eden Prairie, MN) equipped with a 250 N load cell. The specimens were loaded at a crosshead speed of 0.2 mm/min until fracture. The flexural strength was calculated using the maximum compressive load, P, applied by the platens of the MTS perpendicular to the line raster orientation in the samples. A total of 10 specimens were tested for each suspension composition in order to measure an average flexural strength.

A two-tailed *t*-test was used to confirm a statistical significance of average grain sizes, mechanical properties, and densities of the alumina samples. An *F*-test was first used on the data set to determine whether the variances were equal or not, which determined whether a *t*-test with equal variances or a *t*-test for nonequal variances was used. Both the *F*-test and *t*-tests were calculated using Microsoft Excel functions, and data sets were considered statistically significant if $P < 0.05$.

Results and Discussion

Flow curves for the alumina suspensions are shown in Fig. 2 and show that all suspensions act as yield-pseudoplastic fluids with curve parameters fitting the Herschel–Bulkley model (correlation factor $R^2 \sim 0.99$) shown in Table I. The yield-pseudoplastic behavior is attributed to a loosely flocculated structure with a particle network.[19] Previous research on similar highly loaded alumina suspensions found no rheological time dependence of the suspensions, so thixotropy studies were excluded from the present work.[11] These previous studies also investigated the flow behavior up to 100/s and found no change in a uniform yield-pseudoplastic behavior at shear rates excess of the 35/s studied here.[10,11]

An increase in both viscosity and yield stress is observed for suspensions with increasing solid loading. This is attributed to the decreased distance between particles that occurs with an increase in particle content, leading to particle collisions and agglomeration. The suspension with the highest solid loading, 58 vol.% alumina, had the highest yield point and viscosity observed, making it the most difficult suspension to extrude as the syringe tip would dry and clog easily. The 51 vol.% alumina suspension had the lowest yield point and viscosity due to the decrease in frequency of particle collisions.[6] This lower viscosity allowed it to flow easily from the syringe, but did not support each subsequent deposited layer well. The 53, 55, and 56 vol.% suspensions had intermediate viscosities and yield stresses and were optimal for direct writing as they flowed easily from the syringe and were viscous enough to support multiple deposited layers of complex structures. These suspensions were the compositions of alumina suspensions that were further examined in this study for density, microstructure, and mechanical properties due to their desirable flow properties.

As previously mentioned in Section Rheological characterization in Experimental Approach, the 53–56 vol.% alumina suspensions experienced a maximum shear rate (at the syringe walls) ranging from 19.5 to 24.2/s. This shear rate corresponded to viscosities ranging from 9.9 Pa·s for the 53 vol.% alumina suspension to 17.2 Pa·s for the 56 vol.% alumina suspension (viscosity curves for each suspension are shown in Fig. 3). Shear rates were also measured for the suspensions that were determined to be unsuitable for direct writing, 51 and 58 vol.% alumina. The 51 vol.% alumina suspension experienced a maximum shear rate of 25.3/s during extrusion, corresponding to a viscosity of 7.5 Pa·s. The 58 vol.% alumina suspension experienced a maximum shear rate of 15.8/s, corresponding to a viscosity of 25.0 Pa·s. Ideal viscosity for optimal machine parameters applied to these alumina suspensions was nominally between 8 and 20 Pa·s, as shown in Table III. The yield stresses for the suspensions studied, shown in Table I, range from 116 Pa for the 53 vol.% suspension to 191 Pa for the 56 vol.% suspension. The 51 and 58 vol.% alumina suspensions that were found unsuitable for the process had yield stresses of 83 and 268 Pa, respectively.

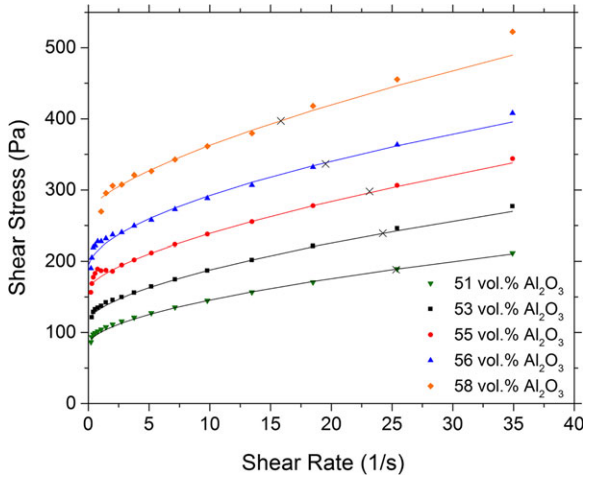

Fig. 2. Flow curves for alumina suspensions with varying alumina solid loading. Curve fits to the Herschel–Bulkley fluid model are shown as solid lines with $R^2 > 0.98$. The 51 and 58 vol.% alumina rheology was found unsuitable for direct writing. An "x" denotes the nominal shear stress during extrusion for each suspension based on shear rate calculations.

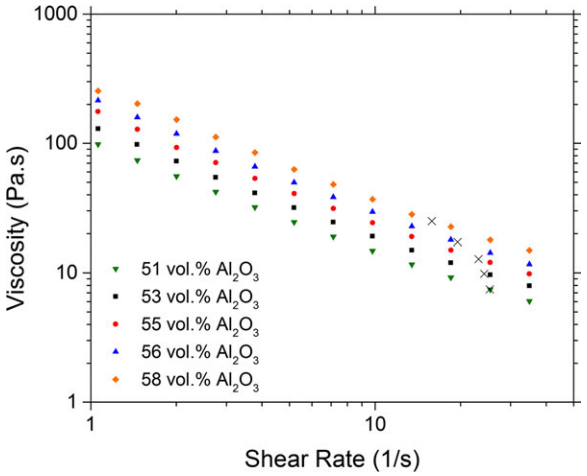

Fig. 3. Log viscosity against log shear rate plots of alumina suspensions prepared with varying alumina solid loading. An "x" denotes the nominal viscosity during extrusion for each suspension.

Table III. Summary of Optimized Suspensions and Parameters for Direct Writing of Aqueous Alumina Suspensions. Nominal Viscosity During Forming was Calculated Based on Measured Shear Rates During Forming for Each Suspension, and Average Layer Height was Measured from Green Body Specimens Formed via Direct Writing

Al_2O_3 (vol.%)	Shear Rate during forming 1/s	Nominal viscosity during forming (Pa·s)	Rheology suitable for printing?	Slumping after deposition?	Average deposited layer height (mm)	Layer uniformity suitable for optimum parts?
51	25.3	7.5	NO	YES	0.88 ± 0.37	NO
53	24.2	9.9	YES	NO	0.85 ± 0.14	NO
55	23.2	12.8	YES	NO	0.85 ± 0.07	YES
56	19.5	17.2	YES	NO	0.90 ± 0.20	NO
58	15.9	25.0	NO	NO	0.86 ± 0.32	NO

Stuecker *et al.*[6] used robocasting as a method to direct write aqueous mullite suspensions with yield-pseudoplastic rheology and a reported yield stress of 30 Pa. While shear rates during deposition were not reported, a tip with a diameter of 1.19 mm was used (similar to the 1.26 mm size used in the current study), but viscosities were much lower ranging from 0.1 to 1 Pa·s for shear rates of 1–500/s.[6] The higher yield stresses and viscosities of the current study are likely due to a different ceramic system with an over three times smaller average particle size of the alumina used. Morissette *et al.* similarly used the robocasting process but with aqueous alumina gel casting suspensions with a wide range of syringe tip diameters (0.254–1.37 mm) and starting ceramic particle size similar to that used in this study. For their tip size of 1.37 mm, their calculated shear rate during forming was 33.5/s.[20] Their reported viscosity for an 45 vol.% solid loading suspension at this shear rate was approximately 2.5 Pa·s,[20] similar in magnitude to the optimized values of the current study shown in Table III.

A forming study was conducted, along with the previously discussed rheology results in Section 3.1, to determine the suspensions with optimal extrusion properties for the direct writing process. A summary of the optimization of specimens based on rheology and part uniformity is outlined in Table III. The shape of the part formed via direct writing is shown in Fig. 1b. This test shape was created to test multiple forming geometries, including a 90° turn, a large radius of curvature, a series of smaller radii curves, and a 3-cm-long straight section. Figure 4 shows a side view of 10 extruded layers of each alumina suspension studied, taken from the 3-cm-long straight section in the test shape shown in Fig. 1b. These green bodies had been completely dried at room temperature for <2 h. The long straight section affords assessment of how well each suspension can support its own weight during forming.

Slumping in the section shown in Fig. 4 indicated that the lower, or first formed, extruded layers were unable to support subsequent layers. Slumping was observed only in the 51 vol.% alumina suspension, as evidenced by bowing of layers 4 through 10 out of plane parallel to extruded direction. This is due to the low yield stress of the 51 vol.% alumina suspension. Research on similar yield-psuedoplastic suspensions used for direct writing found that the yield stress of the extrudate must be such that the deposited layers do not exceed the yield stress upon deposition, causing relaxation and deformation.[6] In the case of the current study, the stress of the added deposited layers must have exceeded approximately 83 Pa, the yield stress of the 51 vol.% alumina suspension.

While slumping was only observed in the 51 vol.% alumina suspension, clumping and uneven extruded layer height were observed in the 58 vol.% suspension making it also undesirable for direct writing. This nonuniformity was due to the drying of suspensions and build-up in the syringe tip due to its higher viscosity and lower water content. The 53–56 vol.% alumina suspensions were best for direct writing as they experienced no slumping, and had relative uniformity between successive layers of the extrudate. It can be observed in Fig. 4 that the 55 vol.% suspension was the optimal suspension as it demonstrated the most uniformity in layers. The average layer height for each suspension is shown in Table I and was measured from specimens shown in Fig. 4. These average layer heights are plotted as a function of solid loading in Fig. 5. While there was no statistical significance between the layer heights, the standard deviation in heights was much larger for the 51 and 58 vol.%

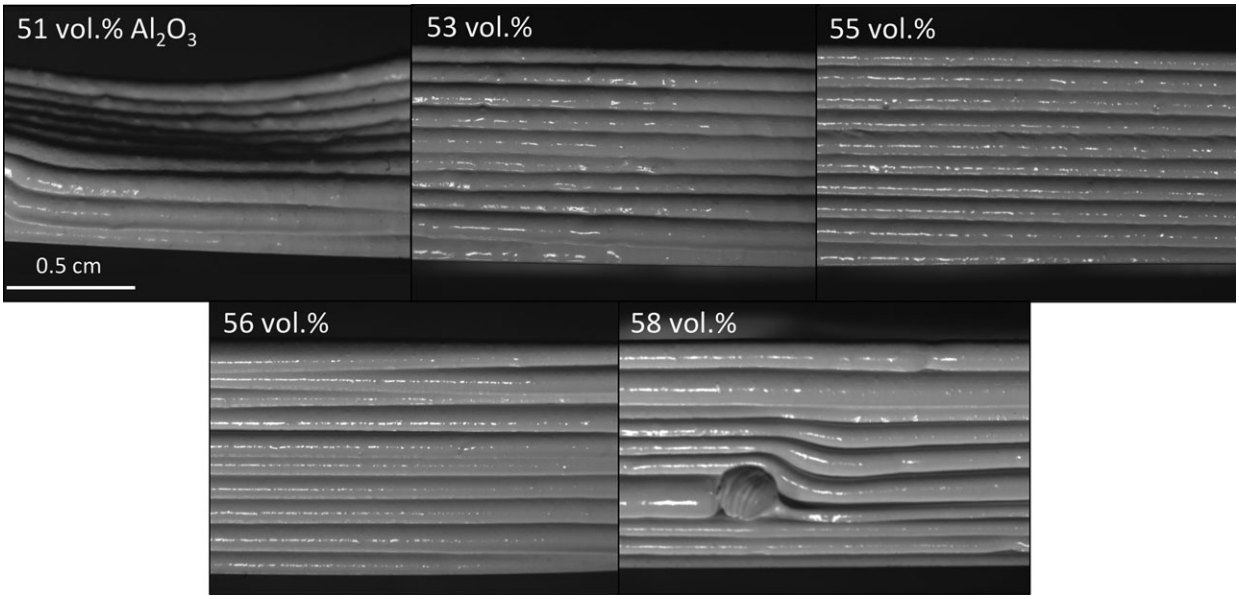

Fig. 4. Side view of green bodies formed via direct writing 10 layers for each of the alumina suspensions tested. These sections were taken from the straight edge of the test shape shown in Fig. 3.

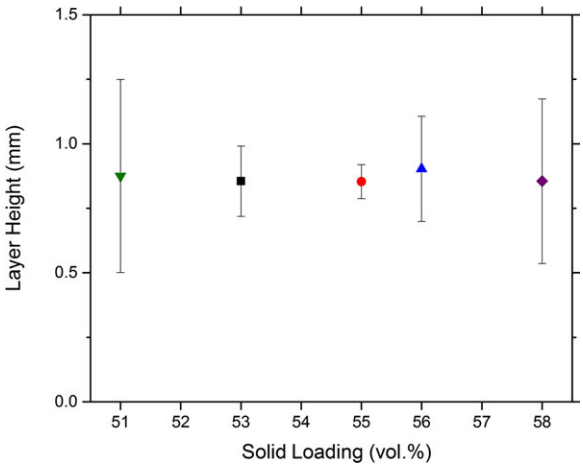

Fig. 5. Average layer height measured from the side view of two green bodies for each of the alumina samples tested. There is no statistical significance between the average layer heights of each sample, while the standard deviation reveals the greatest discontinuity in layers with the 51 and 58 vol.% suspensions.

alumina suspensions as compared to the 55 vol.% suspension. The low standard deviation for this sample confirms the high uniformity in extruded layers and is therefore most desirable for this process. This is reflected in the optimization table shown in Table III.

Finally, Fig. 6a shows the sintered specimen that was formed through direct writing a 55 vol.% alumina suspension (the green body shown in Fig. 1b). A cross section of this sintered piece is shown in Fig. 6b with visible adhesion between subsequent deposited layers with no porosity along the interface between layer 1 and layer 2.

The linear shrinkage that occurred during drying for the samples was <0.2%, independent of alumina solid content. The calculated geometric green body density in a dry condition of representative specimens made from 56 vol.% alumina suspensions was 1.96 ± 0.03 g/cm^3, which corresponds to a packing factor of 0.55 ± 0.01 when taking into account the remaining constituents. This packing factor is approximately equal to the starting solid loading of the alumina suspension, and it is expected that all specimens have packing factors equal to the starting solid content in the suspension.

Sintered density results shown in Table IV, obtained through Archimedes testing (ASTM 373[17]), three mechanical test specimens made from each suspension, confirmed samples were all sintered to ~98%TD regardless of alumina content. A two-tailed *t*-test confirmed that there was no statistical difference between the densities, meaning there was no dependence of alumina powder content on final sintered density.

A representative SEM microstructure taken from a polished and thermally etched sample assembled by direct writing a 55 vol.% alumina suspension is shown in Fig. 7. The SEM analysis showed overall dense microstructures with porosity observed mainly on grain

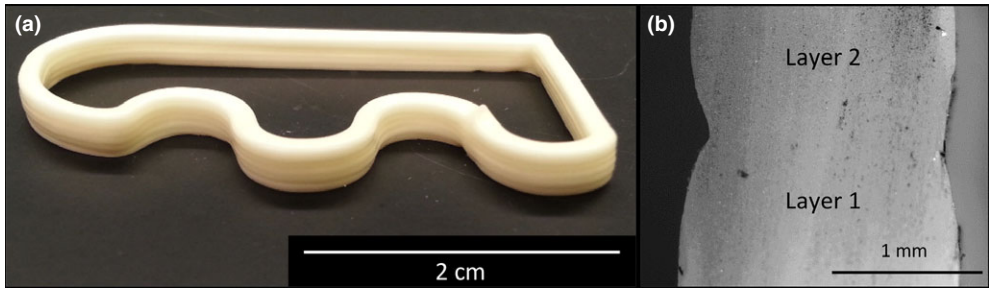

Fig. 6. Test shape formed by room-temperature direct writing of a 55 vol.% alumina suspension (a) after binder removal and sintering. (b) Cross section of the sintered piece acquired via optical microscopy shows adhesion between subsequent deposited layers of alumina suspension.

Table IV. Average Sintered Bulk Density, Average Grain Size, and Average Flexural Strength for Sintered Samples Made Through Direct Writing Alumina Suspensions

Al_2O_3 (vol.%)	Average Sintered Bulk Density (g/cm^3) [%TD]	Average Grain Size (μm)	Average Flexural Strength (MPa)
51	N/A	N/A	N/A
53	3.90 ± 0.03 [98.1]	3.49 ± 0.44	147.5 ± 11.2
55	3.90 ± 0.01 [98.0]	3.17 ± 0.37	156.6 ± 17.5
56	3.91 ± 0.01 [98.2]	3.71 ± 0.37	133.6 ± 17.8
58	N/A	N/A	N/A

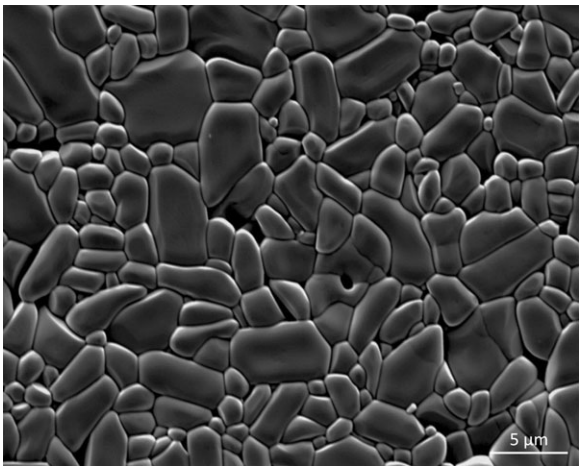

Fig. 7. SEM micrograph of a representative cross section of a sintered and thermally etched alumina specimen prepared by room-temperature direct writing. A small amount of porosity is observed, most often seen on grain boundaries.

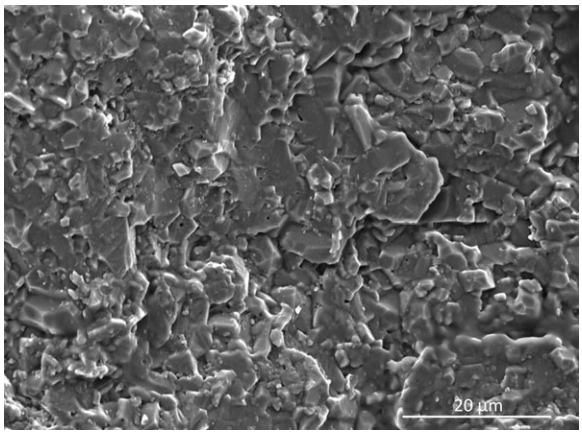

Fig. 8. A representative tensile fracture surface for a sintered 55 vol.% alumina suspension. Mostly transgranular fracture is observed, with no delamination between deposited filament layers.

boundaries in all observed samples. The mean grain sizes for each suspension tested are highlighted in Table IV and ranged from 3.2 to 3.7 μm. Mean grain sizes were shown to be smallest for the parts made with 55 vol.% alumina suspensions. Applying a two-tailed *t*-test proved that the mean grain size for the 55 vol.% specimen was statistically smaller than the 53 and 56 vol.% specimens since $P < 0.05$ ($P_{55vol.\%,\ 53vol.\%}$ = 0.012E-4 and $P_{55vol.\%,\ 56vol.\%}$ = 0.059E-14).

A representative fracture surface of the deposited alumina is shown in Fig. 8. The fracture surface was transgranular with no apparent preferential cracking

between each deposited layer formed during direct writing. Microstructural analysis of sintered cross sections (not shown) of the mechanical test specimens revealed porosity of a bimodal distribution with porosity sizes 0.26 ± 0.08 mm and 0.76 ± 0.08 mm. It is hypothesized that the smaller pores are introduced during mixing, while the larger pores are introduced during filling of the syringe.

The calculated values for average flexural strength were determined using ASTM C1161[18] for samples formed via direct writing 53, 55, and 56 vol.% alumina suspensions. The average flexural strength values are shown in Table IV. Applying a two-tailed *t*-test confirmed that the mean flexural strength of 156.6 MPa for the 55 vol.% alumina specimens was statistically larger than the average strength of 133.6 MPa for the 56 vol.% specimens since $P < 0.05$ ($P_{55\text{vol.\%},\ 56\text{vol.\%}} = 0.022$). However, there was no statistically significant relationship between the 55 vol.% and 53 vol.% samples since $P > 0.05$ ($p_{55\text{vol.\%},\ 53\text{vol.\%}} = 0.226$). There is evidence to suggest the peak flexural strength of the 55 vol.% samples is related to the statistical significant minimum in average grain size of the same composition. The Hall–Petch relationship observes that for small grains there is no variation in strength with grain size, while strength decreases at larger grain sizes (or when flaw and grain sizes are comparable).[21] While the Hall–Petch relationship was first observed in polycrystalline metals, it has been observed in all material systems, including a study by Krell *et al.*[22] that found high-purity alumina to exhibit an increased potential for higher strengths with decreasing grain size.

Previous work using similar aqueous alumina suspensions to the current study were formed via injection molding and sintered to ~98% density.[10] However, average strength values of 192 ± 27.2 MPa were measured with a C-ring test rather than a 3 point bend test.[10] Huang *et al.*[4] used aqueous-based freeze-form extrusion fabrication as a layer-by-layer technique to form alumina specimens with 98% density after sintering and flexural strength values ranging from 150 to 327 MPa. Gel casting was used by Young *et al.*[13] to form alumina parts sintered to 86–99% density with flexural strengths of 248 ± 42 MPa. The average flexural strengths in the current study ranged from 134 to 157 MPa and are at or below the reported values discussed, likely due to the homogenously distributed pores seen throughout the cross section that likely acted as crack initiation sites. Although there is significance in the grain sizes statistically, it is believed that the pores present in the structure dominate the fracture strength of the material. Further research will investigate ways to eliminate porosity both during mixing and syringe filling through using a planetary mixer.

Summary and Conclusions

A process has been established to fabricate near-net shaped dense ceramic components via room-temperature direct writing of highly loaded aqueous ceramic suspensions. This process combined previously established direct writing additive manufacturing techniques with the unique processing capabilities enabled by the flow properties of these suspensions that contain a water-soluble polymer allowing for robust and machinable green bodies. The effect of alumina solid loading on rheology, uniformity of formed parts, density, microstructure, and mechanical properties were studied. Rheology as well as sintered part properties was investigated as related to the direct writing process. Viscosity or shear stress ranges were established for successful extrusion as a function of nozzle diameter in this study. Average flexural strengths were lower than expected but were determined to be largely effected by the porosity introduced during mixing of the aqueous suspensions. The etched micrographs confirmed very little porosity in grains and at grain boundaries due to incomplete sintering, and fracture surfaces show no delamination or preferential cracking between deposited layers. There was no relevant difference found in the material properties (e.g., density and grain size) and mechanical properties with respect to solid loading. Future work will include evaluating alternate mixing approaches for the suspensions and methods of loading syringes to obtain more uniformly mixed suspensions and therefore parts with improved properties. This unique direct writing process that takes advantage of the room-temperature flow properties, along with green body strength, of these suspensions will be investigated as a technique for fabricating more complex geometries ranging from overhanging structures to ceramic matrix composites using two-phase suspensions or two separate ceramic suspensions.

Acknowledgments

The authors would like to thank the U.S. Army Research Office (Grant #W911NF-13-0425) and the U.S. National Science Foundation (Graduate Research Fellowship Program Grant #DGE-1333468) whom both supported this work. The authors are also thankful to Professor Carlos Martinez at Purdue University for the use of his rheometric equipment.

References

1. N. Guo and M. C. Leu, *Front. Mech. Eng.*, 8 [3] 215–243 (2013).
2. J. A. Lewis, J. E. Smay, J. Stuecker, and J. Cesarano III, *J. Am. Ceram. Soc.*, 89 [12] 3599–3609 (2006).
3. M. Allahverdi, S. C. Danforth, M. Jafari, and A. Safari, *J. Eur. Ceram. Soc.*, 21 1485–1490 (2001).
4. T. Huang, M. S. Mason, X. Zhao, G. E. Hilmas, and M. C. Leu, *Rapid Prototyp. J.*, 15 [2] 88–95 (2009).
5. K. Cai, D. Guo, Y. Huang, and J. Yang, *J. Eur. Ceram. Soc.*, 23 [6] 921–925 (2003).
6. J. N. Stuecker, J. Cesarano, and D. A. Hirschfeld, *J. Mater. Process. Technol.*, 142 [2] 318–325 (2003).
7. J. Cesarano, *MRS Proc.*, 542 133–139 (1998).
8. J. A. Lewis, *Curr. Opin. Solid State Mater. Sci.*, 6 [3] 245–250 (2002).
9. J. A. Lewis and G. M. Gratson, *Mater. Today*, 7 [7-8] 32–39 (2004).
10. V. L. Wiesner, J. P. Youngblood, and R. W. Trice, *J. Eur. Ceram. Soc.*, 34 [2] 453–463 (2014).
11. M. Acosta, V. L. Wiesner, C. J. Martinez, R. W. Trice, and J. P. Youngblood, *J. Am. Ceram. Soc.*, 96 [5] 1372–1382 (2013).
12. V. L. Wiesner, L. M. Rueschhoff, A. I. Diaz-Cano, R. W. Trice, and J. P. Youngblood, *Ceram. Int.*, 42 [2] 2750–2760 (2016).
13. A. C. Young, O. Ornatete, M. A. Janney, and P. A. Menchhofer, *J. Am. Ceram. Soc.*, 74 [3] 612–618 (1991).
14. N. G. McCrum, C. P. Buckley, and C. B. Bucknall, The Flow of Polymer Melts, in *Princ. Polym. Eng.*, 2001, pp. 304–315.
15. W. Herschel and R. Bulkley, *Colloid J.*, 39 [19] 291–300 (1926).
16. T. F. Tadros, *Rheology of Dispersions: Principles and Applications*, 1st edition. Wiley-VCH Verlag GmbH & Co. KGaA, Weinheim, Germany, 2010.
17. *Standard Test Method for Water Absorption, Bulk Density, Apparent Porosity, and Apparent Specific Gravity of Fired Whiteware Products*; in ASTM C373-88. ASTM International, West Conshohocken, PA, 2006.
18. *Standard Test Method for Flexural Strength of Advanced Ceramics at Ambient Temperature*; in *ASTM C 1161-02c*. ASTM International, West Conshohocken, PA, 2008.
19. J. E. Smay, J. Cesarano, and J. A. Lewis, *Langmuir*, 84 [18] 5429–5437 (2002).
20. S. L. Morissette, J. A. Lewis, J. Cesarano, D. B. Dimos, and T. Baer, *J. Am. Ceram. Soc.*, 83 [10] 2409–2416 (2000).
21. R. W. Rice, Machining Flaws and the Strength Grain Size Behavior of Ceramics; in *Sci. Ceram. Mach. Surf. Finish.*, 1979.
22. A. Krell and P. Blank, *J. Ceram. Soc. Japan*, 16 1189–1200 (1996).